JOURNAL OF MATERIALS SCIENCE 29 (1994) 6485–6494

Solid-state deformation of polytetrafluoroethylene powder

Part I *Extrusion drawing*

H. OKUYAMA, T. KANAMOTO
Department of Applied Chemistry, Science University of Tokyo, Kagurazaka, Shinjuku-ku, Tokyo 162, Japan

R. S. PORTER
Polymer Science and Engineering, University of Massachusetts, Amherst, MA 01003, USA

Polytetrafluoroethylene (PTFE) powder of a high molecular weight ($\sim 10^7$) was drawn by solid-state extrusion in the temperature range 100–340 °C, which covers the glass transition temperature (125 °C) and the ambient melting point (334 °C). Draw was attainable only above 100 °C. The maximum achievable extrusion draw ratio (EDR_{max}) was almost constant, ~ 10, from 100–280 °C, yet increased rapidly with further increasing temperature, reaching a maximum of 60 at 330–340 °C. At yet higher temperatures, the drawability was lost due to melting. The structure and properties of drawn products were found to be complexely affected by extrusion temperature and EDR. For extrusion at 330–340 °C, near the melting point, an effective and high draw was achieved. The crystalline chain orientation function, crystallite sizes, both along and perpendicular to the chain axis, differential scanning calorimetry heat of fusion, and flexural modulus increased with EDR and approached a maximum at EDR of 30–40, depending on the extrusion temperatures. Above a specific EDR, the efficiency of draw decreased due to the formation of flaws. The highly oriented PTFE consisted of microfibrils of a significantly large lateral dimension (~ 45 nm) compared to those (6–20 nm) generally found in oriented polymers. The modulus of a drawn PTFE was sensitive to the test temperatures, reflecting the reversible crystal/crystal transitions at ~ 19 and 30 °C. The optimization of the extrusion conditions resulted in the maximum achieved flexural modulus at 24 °C of 20 GPa at an EDR 40 for extrusion at 340 °C.

1. Introduction

Solid-state deformation of semicrystalline polymers has been extensively studied to produce high-performance morphologies by uniaxial and biaxial drawing [1–3]. It has been shown [4] that highly drawn polyethylene, polypropylene, and poly(4-methyl-1-pentene) of high molecular weights, exhibit tensile moduli close to the theoretical values for each of these polymers. The morphology of such extreme samples has also been studied and reviewed [5–9]. The gel spinning/drawing technique [10] of ultrahigh molecular weight polyethylene (UHMW-PE), invented by Smith *et al.*, has become an industrial process for the production of extremely high modulus/strength fibres, 3 GPa. More recently, Smith *et al.* [11, 12] proposed a new route to high modulus/strength fibres by ultradrawing of virgin UHMW-PE prepared under controlled conditions. Independently, we have also shown that compacted powders, of virgin UHMW-PE [13–15] and polyacrylonitrile [16], in the forms of billets and films, were effectively ultradrawn by several techniques, including solid-state extrusion [13], coextrusion [14], and two-stage drawing [15] which consists of the first solid-state coextrusion followed by tensile drawing.

Virgin PTFE prepared by emulsion polymerization consists of different morphologies, i.e. spherical particles, rods [17, 18] and needle-like whiskers [19]. Independent of such differences, these particles have been shown to be highly crystalline and have a chain-extended conformation. Starkweather [20] has shown, in his rheological study of PTFE, that continuous and oriented fibres were produced on solid-state extrusion of virgin powder of PTFE. Gee and Collier [21] have studied the effect of extrusion conditions on the tensile properties at room temperature of extrudates prepared at 250–300 °C, and having an extrusion draw ratio (EDR) of 55.8. They concluded that the maximum tensile properties at this constant EDR were obtained for extrusion at 300 °C and at the highest pressure of ~ 100 MPa.

In this work, we have studied the effects of extrusion variables on the deformation behaviour of PTFE powder of commercial grades. The structure and properties of the initial powder and the resultant drawn products have been characterized by several

0022–2461

techniques, including wide-angle X-ray diffraction, scanning electron microscopy (SEM), differential scanning calorimetry (DSC), density, and flexural modulus. The complex variations in morphology and properties with extrusion temperature and sample EDR are discussed.

2. Experimental procedure

2.1. Polymer

The preliminary examination of the drawability of four as-received PTFE powders of commercial grades, which were provided by Mitsui/Du Pont Fluorochemicals, showed that the grade 800-J was most ductile. Thus, this grade, prepared by suspension polymerization and coagulated at room temperature [22], was used throughout this work, otherwise stated. The nominal molecular weight was $\sim 10^7$. The as-received PTFE powder had an average diameter of $\sim 600\ \mu m$, and density of $2.282\ g\,cm^{-3}$, corresponding to crystallinity of 95%. The melting point, measured by DSC at several heating rates and extrapolated to a heating rate of $0\ °C\,min^{-1}$, was 334 °C. The powder was compression moulded at $\sim 10\ °C$ below the ambient melting point (334 °C) and at 100 MPa for 30 min, into a billet 1 cm diameter and 7 cm long.

2.2. Extrusion drawing

The compacted powder billets were extruded at constant temperatures of 25–360 °C through brass conical dies having an included entrance angle of 20° and nominal extrusion draw ratio (EDR) of 4–60. No die swell was observed on solid-state extrusion. For extrusion just below the melting point, a pressure of 20–30 MPa was applied on the billet during heating to the extrusion temperature, T_e, to suppress melting.

2.3. Testing

Wide-angle X-ray diffraction (WAXD) photographs were recorded at 14, 24 and 40 °C on a flat plate camera with nickel-filtered CuK_α radiation generated at 40 kV and 30 mA. Diffractometer scans were made at 22 °C on a Rigaku Geigerflex RD-III A, equipped with a pulse height discriminator. The intensity was collected by step scan at 0.01°–0.05° intervals in 2θ, and the counting time was adjusted to accumulate the peak intensity of $\sim 10^4$ counts. The ($h\,k\,0$) reflection profiles were measured by a symmetrical reflection mode, and those of the ($0\,0\,l$) were measured by a symmetrical transmission method. For the former measurements, line collimators of 1/6° (DS), 0.15 mm (RS), and 1/6° (SS) were used. For the latter, line collimators of 0.05 mm (first), 0.15 mm (second), and 0.15 mm (third) were used. The observed profiles were corrected for the broadening due to the instrumental conditions and $K_{\alpha 1}$ and $K_{\alpha 2}$ radiations, by using the Stoke's deconvolution method and Jones' curve-fitting method [23]. The standard materials used for these corrections were the NBS standard silicon powder and a pure aluminium plate (99.99% purity and annealed at 360 °C) for the reflection and transmission modes, respectively. The crystallite size, D_{100}, and paracrystalline disorder, g_2, perpendicular to the (1 0 0) plane (and hence to the chain axis) were determined from the integral breadths, $\Delta\beta(m)$, of the (1 0 0), (2 0 0), and (3 0 0) reflections according to the following equation [23]

$$[\Delta\beta(m)\cos\theta/\lambda]^2 = (1/D_{100})^2 + (\pi^4 g_2^4 m^4)/(d_{100})^2 \quad (1)$$

where d_{100} is the spacing of the (1 0 0) plane, m the order of reflection, and λ the wavelength of Cu$K_{\alpha 1}$ radiation. The crystallite sizes along the chain axis (D_{0015}) were estimated from the integral breadths of the (0 0 1 5) reflection by Scherrer's Equation [23]

$$\Delta\beta(m) = K\lambda/D_{hkl}\cos\theta \quad (2)$$

where K is a constant and 1, when the integral breadth is used.

The azimuthal scans for the (1 1 0) and (0 0 1 5) planes were made using a Rigaku fibre specimen holder. Crystalline chain orientation was evaluated using the Herman–Stein orientation function, f_c.

Densities of as-received powder and solid-state extrudates were measured at 23 °C by a picnometer method using carbon tetrachloride as a filling fluid. The crystallinity, X_c, was calculated assuming a crystal/amorphous two-phase model, and using $\rho_c = 2.30\ g\,cm^{-3}$ [24] and $\rho_a = 2.06\ g\,cm^{-3}$ [25]. DSC measurements were made on a Seiko-Denshi DSC-10, at heating rates of $1–50\ °C\,min^{-1}$. Sample size was 1–3 mg. Melting and crystal/crystal transition temperatures and heats of the transitions were calibrated with lead and benzoic acid.

Flexural modulus was determined from the initial slope of the stress/strain curve measured on a Tensilon tensile tester UTM-100 at 14, 24, and 35 °C, and at a strain rate of $10^{-3}\ s^{-1}$. SEM observations of the surface produced by fracture in liquid nitrogen were made on a Hitachi S-2400.

3. Results and discussion

3.1. Extrusion draw behaviour

The compacted powder billets were white and opaque. The bulk density of the billets was close to the density of the powder, showing that most of voids were removed during compaction of the powder at 325 °C and 100 MPa. Further, X-ray diffraction showed no selective chain orientation in the initial billets. These billets were extruded at constant temperatures of 25–360 °C, which covered the T_g (125 °C) and T_m (334 °C) of the original powder. An efficient draw was attainable between 100 and 340 °C. For extrusion at temperatures below 100 °C, the extrudates exhibited shear fracture. At $T_e \geqslant 350\ °C$, the efficient drawability of the as-received compacted powder billet was lost, and only helical extrudates were obtained, due to melting of the billet, as revealed by the appearance of a lower melting peak at 324 °C on the DSC thermograms of the residual portion of the billets removed without extrusion. It should be mentioned, here, that recently Wadden and Keller [26, 27] have found a narrow temperature window of smooth extrudability for high MW PE in the melt. In this work, however, as

the extrusion of PTFE slightly above the T_m gave no uniform extrudates, we have not studied further the extrusion behaviour of PTFE from the melt. Fig. 1 shows the maximum achieved EDR (EDR_{max}) as a function of extrusion temperature, T_e. The EDR_{max} at $T_e = 100\,°C$ was ~ 10, and remained at this level up to a T_e of 280 °C. For extrusion at $T_e > 280\,°C$, the ductility increased markedly and an EDR_{max} of 60 could be attained at 330 and 340 °C, near the T_m.

A high ductility of the virgin PTFE powders has previously been reported by Starkweather [20] and Gee and Collier [21]. This is likely related to the specific morphology of the powder which has been shown to be highly chain extended and crystalline [17–19]. Aharoni and Sibilia [28] reported that solid-state extrusion for a number of melt-crystallized polymers was possible only at temperatures above a reversible crystal/crystal transition, because the molecular motion in a crystalline phase increases above such a transition. PTFE exhibits several such transitions below its melting point. It takes a triclinic cell (13_6 helix, Type II) below 19 °C, hexagonal (15_7 helix, Type IV) at 19–30 °C, and pseudo-hexagonal (Types I and I′) above 30 °C and below the T_m. The helical conformation of the Types I and I′ above the 30 °C transition becomes increasingly irregular with increasing temperature by the introduction of increasing number of gauche conformers [29, 30]. Further, the translational displacement along the chain axis increases gradually with temperature [31], and then more rapidly $> 125\,°C$, due to the loss of the order in this chain direction, as revealed by WAXD [29, 30] and broad-line NMR [31].

The drawability of PTFE shown in Fig. 1, was not significantly affected by any of the reported crystal/crystal transitions at about room temperature, and rapidly increased with temperature only above 280 °C up to the melting point. This indicates that the high ductility of PTFE near the melting point is generally related to the significantly increased chain mobility [30, 31] and the rapid increase of the chain separation above 260 °C [20]. Gee and Collier [21] reported that the PTFE powder that they used could be drawn to an EDR of 55.8 at a T_e between 250 and 300 °C and at $P_e \leqslant 100$ MPa. The EDR_{max} at $T_e = 250\,°C$ in our experiment was only 12, remarkably lower than the EDR achieved by them [21]. In this work, extrusion at higher EDR resulted in the products with shear fracture. The drawability, in general, is known to be affected by several extrusion variables, including initial morphology, molecular weight, applied pressure, use of lubricant, bulk density of a billet, etc. Although the details of their extrusion conditions and sample are not known, the morphology of samples is likely the major reason for the significant difference in the ductility at 250 °C, observed in this and their [21] experiments. As stated initially, indeed, we have also found that the four commercial grades of PTFE powders examined exhibited different drawability depending on the preparation conditions.

Fig. 2 shows the WAXD patterns recorded at 24 °C for an EDR series prepared at 330 °C. The crystalline

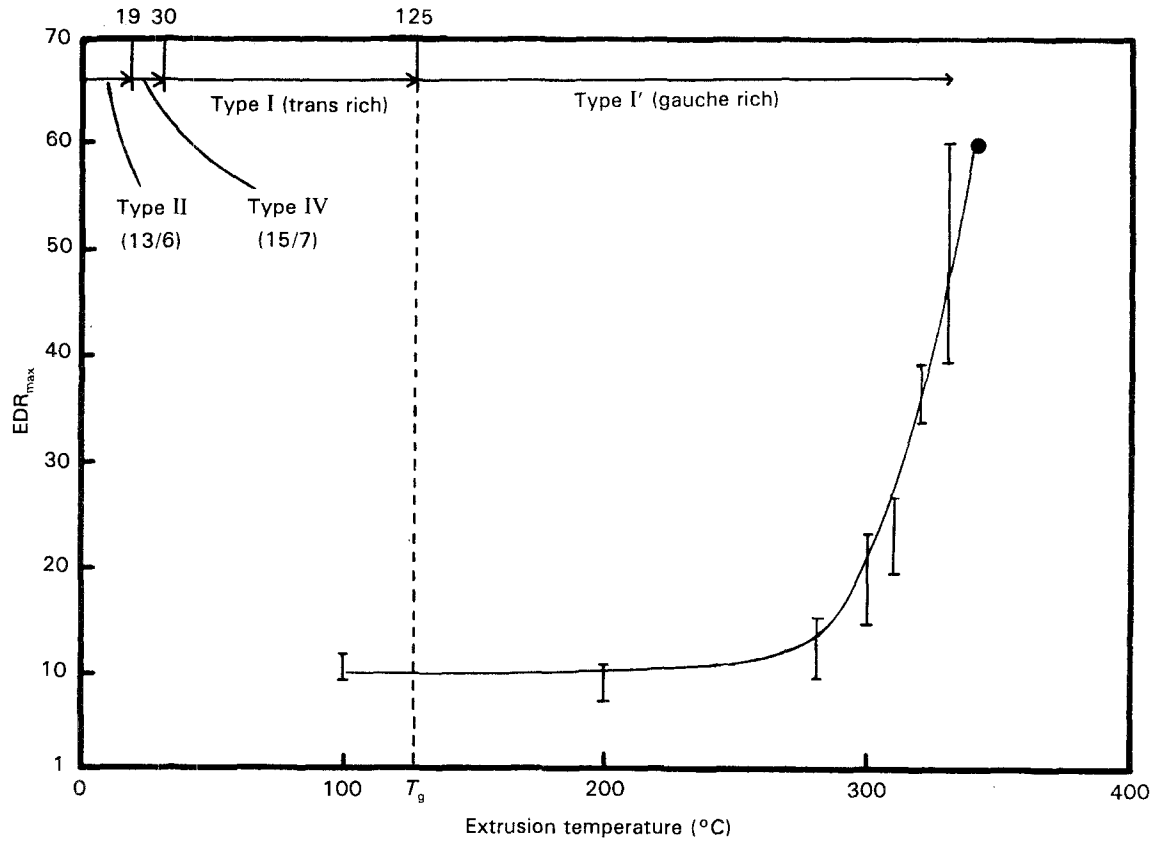

Figure 1 Maximum extrusion draw ratio, EDR_{max}, as a function of temperature for solid-state extrusion of PTFE powder billets. The crystal forms at different temperatures are also indicated.

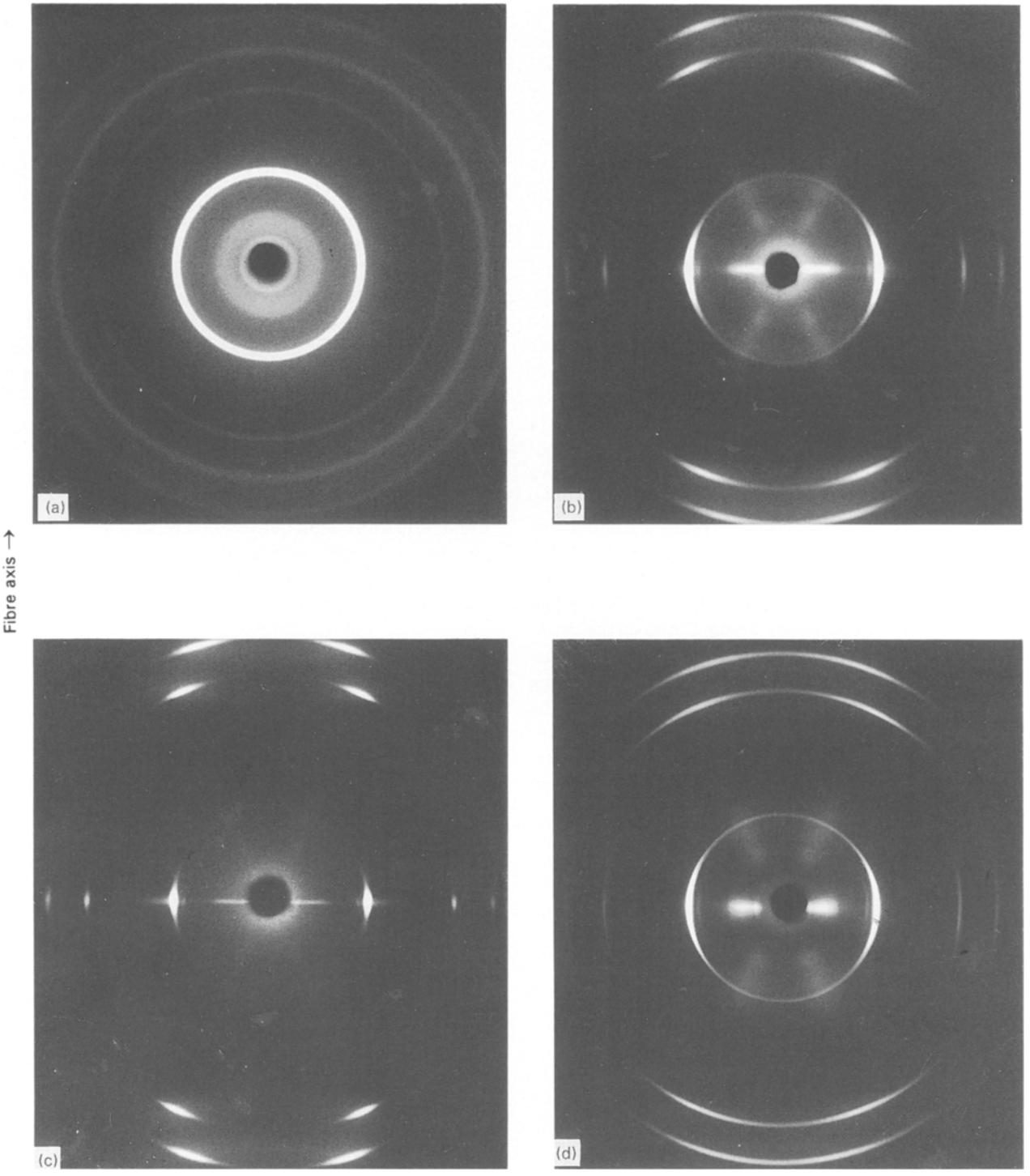

Figure 2 WAXD patterns for a compression-moulded powder billet (a), and for extrudates of EDR (b) 6, (c) 20, and (d) 60, recorded at 24 °C. Extrusion was made at 330 °C.

orientation functions, f_c and f_a, for the chain axis and the a-axis, respectively, are plotted in Fig. 3, as a function of EDR for the extrudates prepared at 100–340 °C. As shown, the chain orientation function, f_c, increased rapidly at lower EDR at each T_e. However, the crystal chain orientation proceeded more rapidly at higher T_e. For extrusion at $T_e = 330$ °C, f_c approached unity at an EDR of 20, yet at higher EDR (> 30–40), it decreased significantly. This is found to be due to the formation of flaws, as observed under an optical microscope. For extrusion at $T_e = 340$ °C, f_c increased in the same way as at $T_e = 330$ °C below an EDR of 20, and stayed almost at unity between an EDR 20 and 40, and then it decreased only slightly to an EDR of 60. These observations, in agreement with other structural features to be described later, show that the generation of flaws in solid-state extrusion of PTFE powder is suppressed at higher temperatures, owing to the increased chain mobility [30, 31] and chain separation [20] as discussed above.

Fig. 4 shows scanning electron micrographs of as-received PTFE powders and surfaces produced on fracture in liquid nitrogen for an EDR series prepared at 330 °C. The original powder of $\sim$ 600 μm diameter, contains a fraction of smaller particles of 0.2–1 μm (Fig. 4a). At an EDR of 6, the initial powder has

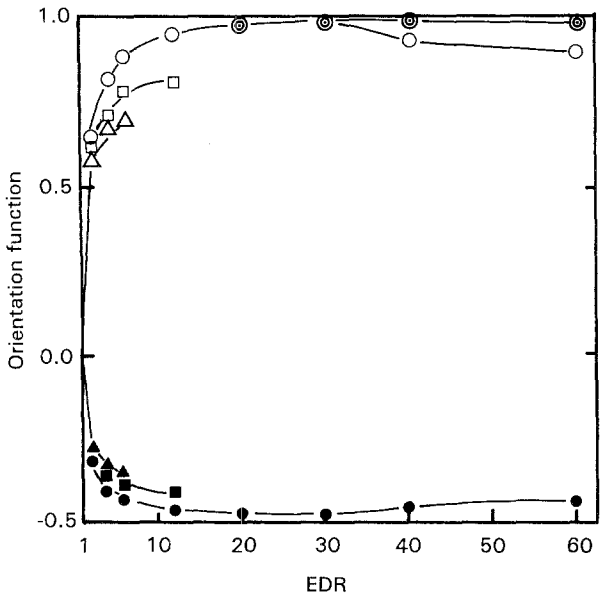

Figure 3 Crystal orientation functions, (⊙, ○, □, △)f_c and (●, ■, ▲)f_a, as a function of EDR for extrusion at (△, ▲) 100 °C, (□, ■) 300 °C, (○, ●) 330 °C and (⊙) 340 °C.

already transformed into an oriented fibrillar morphology (Fig. 4b). With increasing EDR, fibrillation and orientation of fibrils proceeded rapidly, as shown in Fig. 4c and d. The fibrils that connect laterally the well-oriented fibrils were likely formed during fracture of the extrudates, because the WAXD patterns showed no existence of such components. A similar fibrillar structure was also found in the irregular extrudates with flaws prepared at room temperature.

3.2. Melting characteristics and crystallinity

Fig. 5 shows DSC thermograms for an EDR series prepared at 330 °C. The heating rate was 5 °C min^{-1}. The DSC melting curve of a compacted powder billet was identical to that of the initial powder. On extrusion at a low EDR of 6, the melting peak broadened and the peak temperature, T_m, shifted lower. To examine the effect of heating rate on the melting behaviour, DSC scans were made at heating rates of 1–50 °C min^{-1} on the original powder, and on two extrudates with an EDR 6 and 30. Fig. 6 shows the T_m for each sample, which shifted to a higher temperature with increasing heating rate. Both the original powder and a drawn extrudate of an EDR 30 exhibited marked superheating compared to the sample with a lower EDR of 6. However, the trend with heating rate for each EDR was not affected, suggesting no important structural reorganization took place during DSC scans in these samples. Thus, the effects of T_c and EDR on the T_m and heat of fusion of extrudates were determined at a heating rate of 5 °C min^{-1}, and are shown in Figs 7 and 8, respectively. Independent of T_c (100–340 °C), the T_m decreased initially and then recovered gradually at EDR > 6. It is noted that the T_m

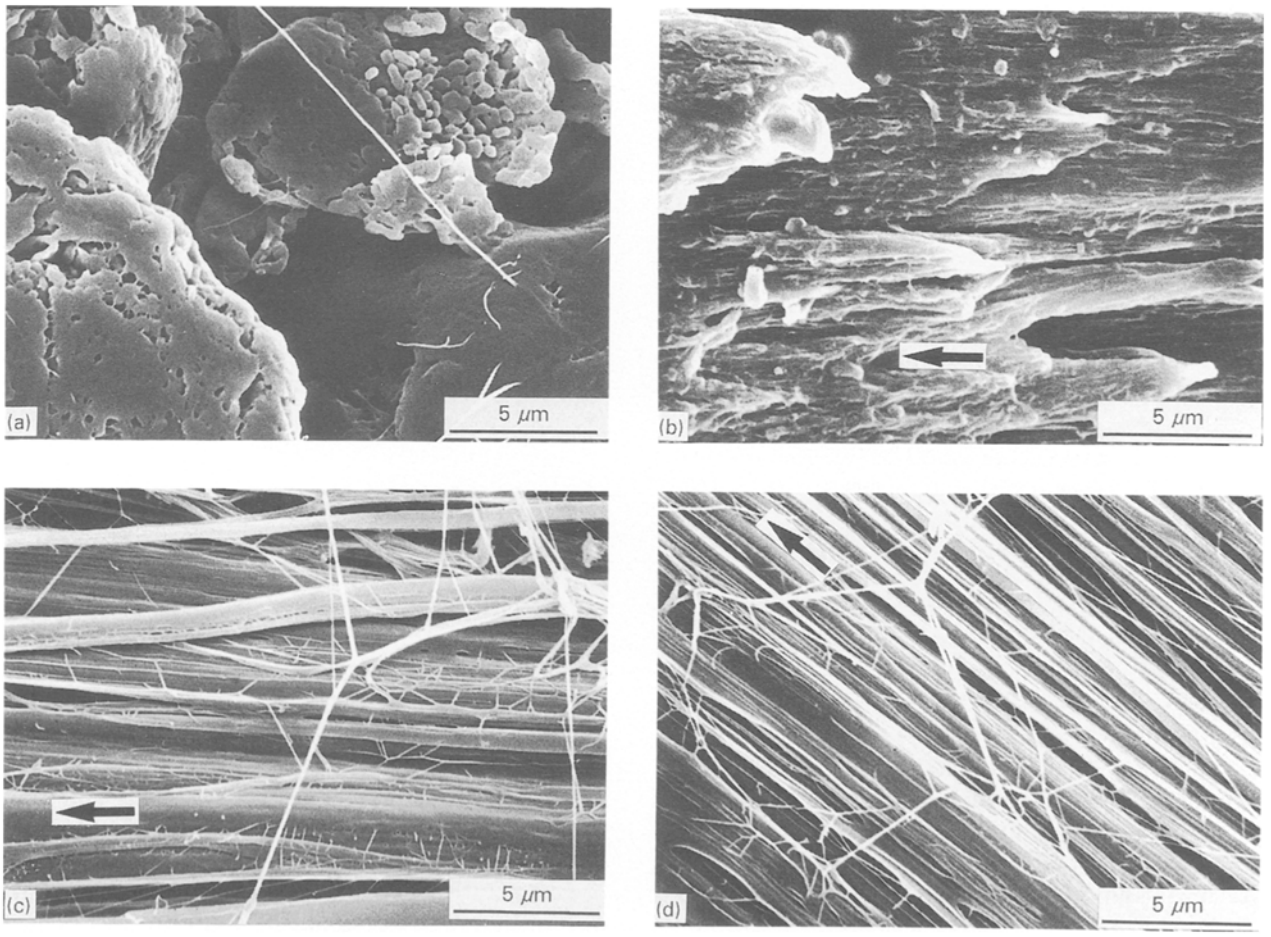

Figure 4 Scanning electron micrographs of (a) as-received powder, and the surfaces produced by fracture of extrudates in liquid nitrogen for EDR (b) 6, (c) 20, and (d) 60. The draw direction is shown by the arrow.

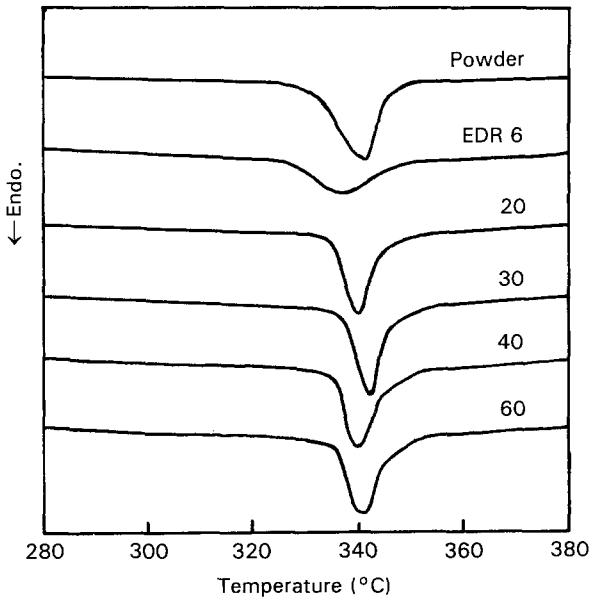

Figure 5 DSC melting thermograms for as-received powder, and extrudates prepared at 330 °C.

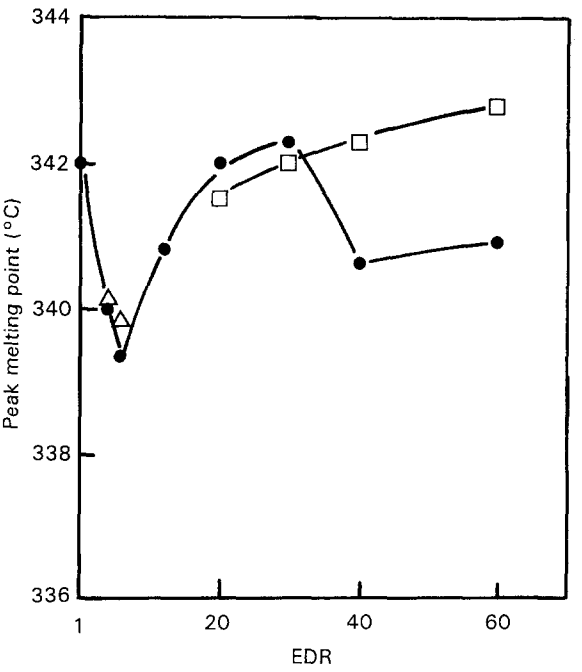

Figure 7 DSC melting peak temperatures as a function of EDR for extrusion at (△) 100, (●) 330 and (□) 340 °C.

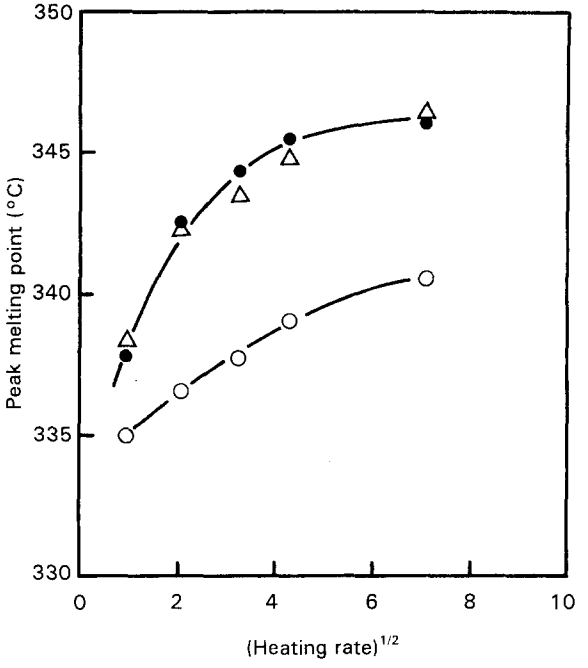

Figure 6 DSC melting peak temperature measured as a function of heating rate for (●) as-received powder, and extrudates of EDR (○) 6 and (△) 30.

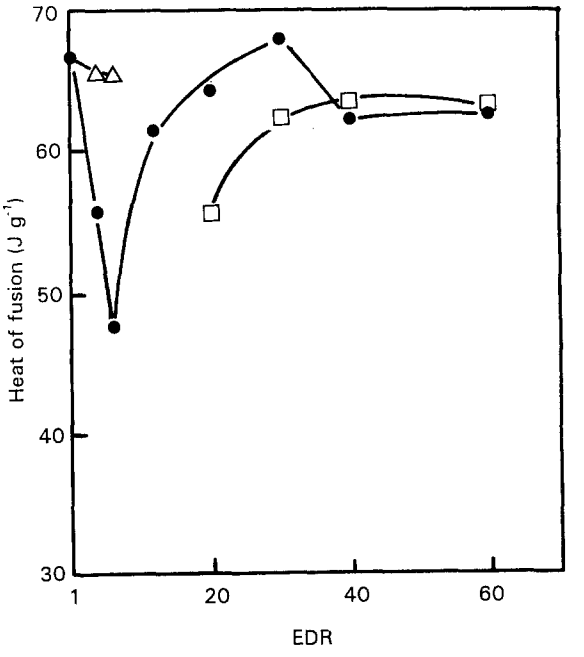

Figure 8 Heat of fusion as a function of EDR for extrusion at (△) 100, (●) 330 and (□) 340 °C.

for extrusion at T_e = 330 °C decreased significantly at high EDR > 30 (Fig. 7). In contrast, no such decrease in T_m at higher EDR was observed at T_e = 340 °C.

The heat of fusion, shown in Fig. 8, changed complexely with T_e and EDR. For extrusion at high temperatures of 330 and 340 °C, the variations with EDR are similar to those found in T_m (Fig. 7). However, the heat of fusion for extrusion at the lowest temperature of 100 °C exhibited no significant decrease at low EDR, where a marked reduction was found for extrusion at higher temperatures approaching the T_m. Such reductions in T_m and heat of fusion at low EDRs were previously found also in solid-state extrusion of ultrahigh molecular weight polyethylene reactor powder [15]. In this case, such behaviour was interpreted as due to the introduction of defects or destruction of the initial crystals. However, it is not clear why the heat of fusion showed no such decrease at low EDRs for extrusion at 100 °C, in spite of the decrease in the T_m. One possibility may be due to the different deformation mechanisms at a low (T_e = 100 °C) and high (330 and 340 °C) temperatures near the T_m. Indeed, Sadler and Barham [32–34] concluded that when drawing of PE was made above a critical temperature, melting followed by recrystallization in an oriented structure occurred, in their recent studies on the neck deformation of HDPE by small-angle neutron

scattering. However, below that temperature, the chain slippage in the crystalline state was a predominant mechanism for the deformation. The deformation by the latter mechanism may not cause a significant decrease in crystallinity.

The variation of crystallinity on draw has also been studied by the sample density measured as a function of EDR. Fig. 9 shows density (crystallinity) as a function of EDR for extrusion at $T_e = 330\,^{\circ}C$. The original powder had a density of 2.282 g cm^{-3}, corresponding to a high crystallinity of 93%. Although the morphology of suspension-polymerized PTFE has not been well studied, such a high crystallinity of the present sample is consistent with the previous studies on the emulsion-polymerized virgin PTFE [17–19]. The density decreased sharply at the initial draw (< 6), and then increased gradually in the higher EDR range, approaching a constant of 2.282 g cm^{-3} at an EDR of 30. Such a change in density is consistent with that found in the heats of fusion measured as a function of EDR (Fig. 8).

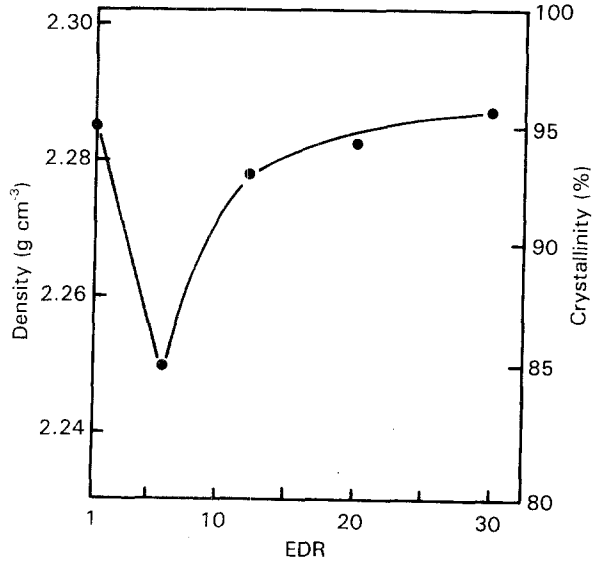

Figure 9 Density of extrudates versus EDR for extrusion at 330 °C, measured at 23 °C.

3.3. Crystallite sizes and disorder

The structural change on draw was further studied by WAXD. Fig. 10 shows crystallite size along the chain direction, D_{0015}, as a function of EDR for extrusion draw at $T_e = 100$, 330 and 340 °C. The compacted powder billet (EDR = 1) showed a D_{0015} of 43.5 nm, remarkably smaller than that anticipated from the previous electron microscopic studies [17–19] which revealed a chain-extended conformation of virgin particles prepared by emulsion polymerization. These suggest that the initially chain-extended crystals might be deteriorated significantly during coagulation of the nascent particles and/or the compression moulding into a billet at a high pressure. This will be discussed later. At a low T_e of 100 °C, the crystallite size, D_{0015}, decreased abruptly on draw from 43.5 nm for EDR = 1 to 34 nm at an EDR of 6. At higher T_es, the D_{0015} increased rapidly in the lower EDR range,

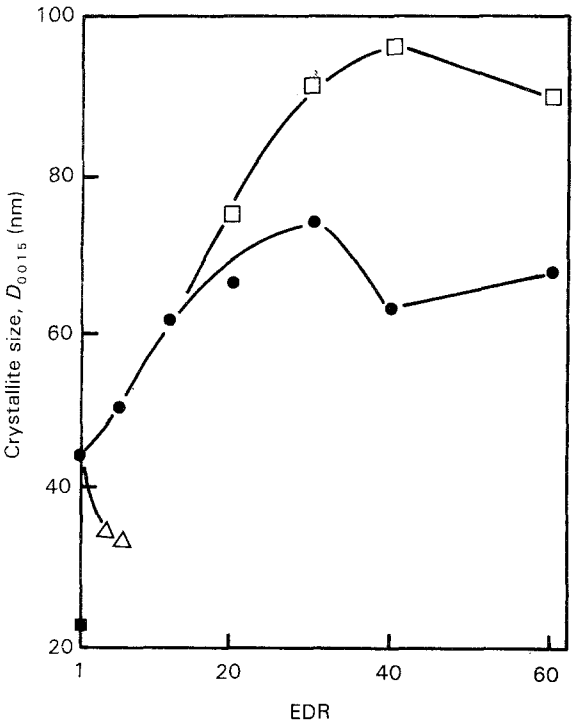

Figure 10 Crystallite size along the chain axis, D_{0015}, versus EDR for extrusion at (△) 100, (●) 330 and (□) 340 °C. The D_{0015} for the as-received powder is also shown (■).

reached maximum values of 75 and 97 nm at $T_e = 330$ and 340 °C, respectively, and finally decreased at higher EDR. Such a critical EDR was higher for extrusion at higher T_e, and the corresponding decrease in D_{0015} was more remarkable at lower T_e. The increase of D_{0015} with EDR can be a measure for the morphological continuity along the fibre axis, as found previously in drawn HDPE [35, 36], and will be discussed later, in relation to the modulus of drawn samples. The reduction in the crystallite size at higher EDR can be ascribed to the formation of flaws, as mentioned. A similar change with EDR was observed in the crystallite sizes perpendicular to the chain axis, D_{100}, as shown in Fig. 11. The decrease in D_{100} was most prominent for extrusion at the lowest T_e of 100 °C. For extrusion at higher T_e, the D_{100} increased with EDR to a constant value of 45 nm at EDR of 20–40, remarkably larger than that generally found in oriented fibres for a number of polymers, including flexible and rigid chain polymers. O'Leary and Geil [37] also observed microfibrils of a comparable lateral dimension in their electron microscopic study on the PTFE surfaces produced by different methods at room temperature. The previous electron microscopic and X-ray diffraction studies on highly oriented polymers report the lateral sizes of crystals or microfibrils in the range of 6–20 nm, for both flexible and rigid polymers. For example, 10–20 nm for PE [35, 36] and PP [38], and 6–10 nm for PPTA [39] poly-*p*-phenyl enebenzobisthiazole (PBT) [40] and polyamides [41]. Although they are slightly affected by the processing conditions, the analysis of the reported data shows a tendency that the size is smaller for the polymers with a higher chain rigidity and stronger intermolecular interactions. PTFE has the weakest intermolecular

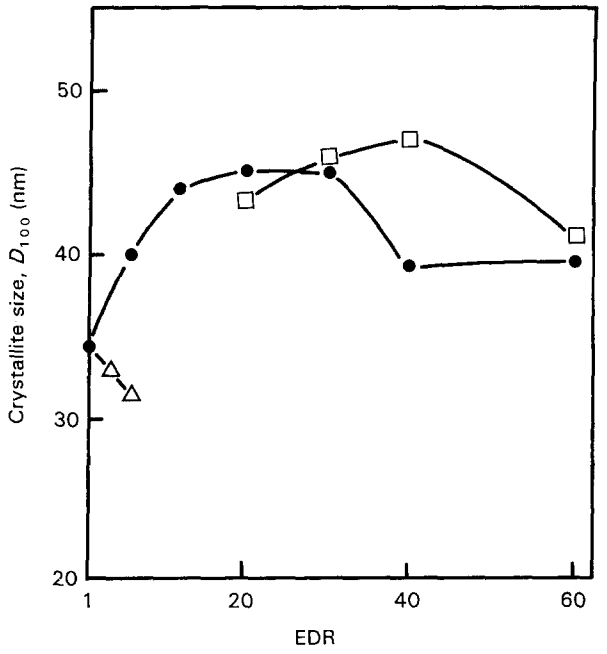

Figure 11 Crystallite size perpendicular to the chain axis D_{100} versus EDR for extrusion at (△) 100, (●) 330 and (□) 340 °C.

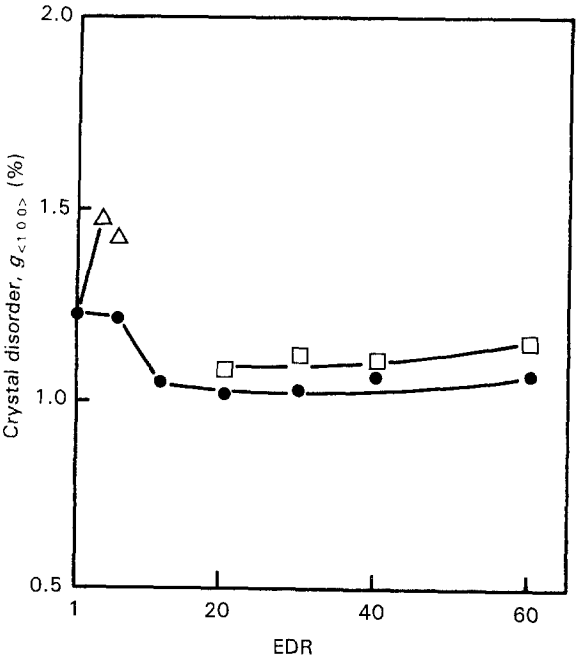

Figure 12 Paracrystalline disorder versus EDR for extrusion at (△) 100, (●) 330 and (□) 340 °C.

forces among polymers. Thus, the larger lateral crystallite size of highly drawn PTFE microfibrils (Fig. 11) is likely related to the characteristic nature of PTFE molecules.

The paracrystalline disorder perpendicular to the chain axis is also shown in Fig. 12 as a function of EDR. At $T_e = 100$ °C, the disorder increased rapidly at low EDR. At the highest T_es of 330 and 340 °C, the disorder decreased at the low EDR, between 6 and 12, and approached a constant of 1.0%–1.1% in the EDR range of 12–60. It is interesting to note that the crystal disorder in the initial billet is slightly larger than that found in the EDR series prepared at 330 and 340 °C. Further, the disorder was not affected by the flaws at high EDR where the crystallite sizes along and perpendicular to the fibre axis both decreased significantly.

3.4. Mechanical property

The modulus of drawn PTFE was found to change sensitively with EDR, T_e, and the test temperature. Fig. 13 shows flexural modulus as a function of EDR for extrudates prepared at 330 °C, measured at 14 °C (triclinic phase), 24 °C (hexagonal phase) and 35 °C (pseudo-hexagonal phase). At a given test temperature, the modulus increased rapidly with EDR in the lower range (EDR $\leqslant$ 30), and reached a maximum at an EDR of 30. However, it decreased abruptly at an EDR of 40, and then slowly at higher EDR. Such a trend in modulus with EDR is consistent with that found in the crystallite size along the chain axis, D_{0015} (Fig. 10) which is a measure of the morphological continuity along the fibre axis. The DSC data in Figs 7 and 8 and f_c in Fig. 3 are also consistent with the variation of modulus with EDR. As discussed above, all of these changes at EDR > 30 for $T_e = 330$ °C have

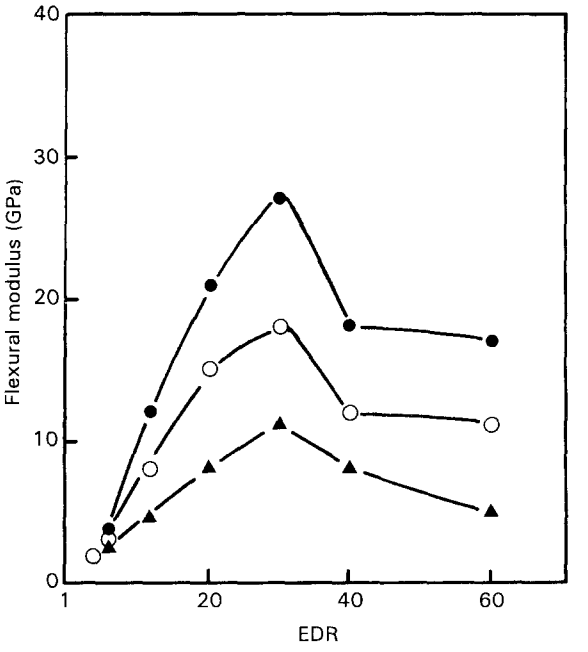

Figure 13 Flexural modulus as a function of EDR measured at (●) 14 °C (Type II, triclinic cell), (○) 24 °C (Type IV, hexagonal) and (▲) 35 °C (Type I, pseudo-hexagonal). The extrusion was made at 330 °C.

been ascribed to the formation of flaws at the higher EDR. The generation of flaws, and hence the sharp decrease in modulus, was found to be affected by T_e as will be discussed later (Fig. 14). At a given EDR, the modulus was sensitive to the test temperature. The maximum achieved flexural moduli for extrusion at $T_e = 330$ °C were 10, 18 and 28 GPa measured at 35, 24 and 14 °C, respectively, at EDR 30. Nishino [29] has shown that the crystal modulus of PTFE drops markedly at ~ 19 and 30 °C ($E_c = 170$ GPa at < 19 °C and 135 GPa at > 30 °C), corresponding to the reversible crystal/crystal transitions. The crystal

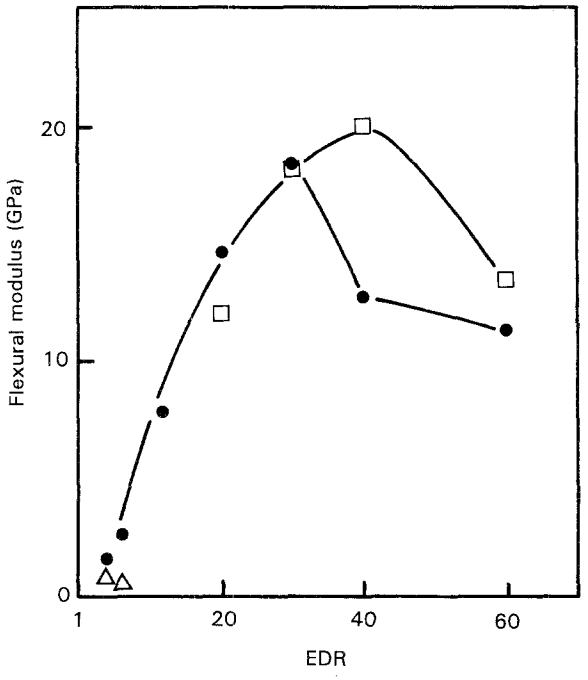

Figure 14 Flexural modulus as a function of EDR for extrusion at (△) 100, (●) 330 and (□) 340 °C. The moduli were measured at 24 °C.

transition temperatures at around room temperature in our samples, measured by DSC and WAXD, were not significantly affected by the EDR of samples.

The increase of modulus with EDR was significantly affected by both T_e and EDR, as shown in Fig. 14. For extrusion at $T_e = 100\,°C$, below the T_g, the modulus showed no increase with EDR, although the EDR range achieved was limited. However, for extrusion at 340 °C, the highest T_e giving an effective draw, the modulus increased rapidly with EDR up to an EDR of 40, which was slightly above the critical EDR of 30 for extrusion draw at 330 °C. As the increase of modulus with EDR, below the critical EDR, was comparable for extrusion at these two T_es, a slightly higher modulus was achieved at $T_e = 340\,°C$ than at 330 °C (20 GPa versus 18 GPa measured at 24 °C).

Chuah and Porter [42] have studied solid-state extrusion of HDPE having a wide range of morphologies prepared by the combination of crystallization temperatures and pressures. They found that the chain-folded crystal morphologies, prepared at relatively low temperatures and pressures gave an effective draw. This was not possible for extrusion of the chain-extended crystals, obtained at a high temperature (221 °C) and pressure (460 MPa). In the latter sample, the deformation proceeded only by slippage along the chain axis in the crystallographic ($h\,k\,0$) planes, producing no connectivity along the deformed crystals. Thus, they concluded that chain folding is a necessary morphological factor in achieving a highly efficient draw of HDPE.

The modulus, as well as other morphological properties discussed above, shows that the PTFE powder used in this work could be drawn with a fairly high efficiency by crystalline-state extrusion up to near the ambient melting point. The morphology of virgin PTFE has been extensively studied for emulsion polymerized samples. Different types of crystalline particles, such as folded ribbons [17, 18], rods [17, 18] and needle-like whiskers [19], have been found depending on the polymerization conditions. It has been concluded that all of these crystals have basically extended-chain conformation, independent of the appearances. In contrast to the emulsion-polymerized PTFE, the morphology of suspension-polymerized one is not clear. The polymerization of our sample was initiated in suspension, but the subsequent reaction proceeded actually in a gas phase. Thus, the crystallization during polymerization might be expected to produce more or less chain-extended crystals, as found in emulsion polymerization [17–19]. However, the present WAXD of the compacted powder billet revealed a small crystallite size along the chain axis ($D_{0015} = 43.5$ nm) and slightly larger crystal disorder perpendicular to the chain axis than in highly drawn extrudates (1.2% versus 1.0%). Thus, we have examined the D_{0015} value for a compacted powder film of a emulsion-polymerized commercial sample (grade 6-J), moulded at the same temperature (325 °C) as that used for the preparation of a billet from the suspension grade (800-J) used in this work. The compacted emulsion grade also showed a small D_{0015} of 38 nm, comparable to that found for the billet of a suspension grade (800-J), and remarkably smaller than that expected from the morphology of nascent particles [17–19]. These features might have resulted from the compression moulding of the powders below the T_m and/or the coagulation treatment of the nascent particles into the as-received powder that we used in this work. To examine the first possibility, the as-received powders were mixed with a small amount of epoxy, and a thin film was prepared. The X-ray examination of this film showed a crystallite size, D_{0015}, of 22 nm, even smaller than that found for the powder billet ($D_{0015} = 43.5$ nm) prepared near the T_m. Thus, the smaller crystallite size observed by X-ray for the as-received PTFE powder is likely related to the significant crystal disorder along the chain axis, induced during the coagulation process of the initially chain-extended, nascent particles. A similarly small crystallite size has been observed in an as-solution-spun fibre of a chain-extended rigid polymer, PBT [26, 27]. Further, the efficiency of draw, as evaluated by the ratio of the sample modulus/the crystal modulus, was significantly lower for the solid-state extrusion of PTFE powder than for that of chain-folded HDPE crystals [36]. For example, at an EDR 30, the moduli of PTFE and HDPE measured at 24 °C were 20 and 45 GPa, corresponding to 13% and 19%, respectively, of the crystal modulus for each of these polymers (158 GPa at 24 °C for PTFE [29], and 235 GPa for HDPE). Moreover, the crystalline orientation function, f_c, at an EDR 30 was 0.997 for HDPE, slightly higher than for PTFE with an f_c of 0.987. Such a lower efficiency of draw, as well as (a) the high T_m (Figs 6 and 7), (b) the high crystallinity (Fig. 9), (c) the remarkable superheating of the PET used here (Fig. 6), and (d) the above consideration of the morphology formation

during polymerization, is consistent with the basically chain-extended morphology with a significant number of defects along the chain axis.

4. Conclusion

PTFE powder, commercial grade, which has never been heated above the T_m, was ultradrawn by solid-state extrusion over a wide range of temperatures between 100 and 340 °C. The EDR_{max} was nearly constant at ~ 10 for a T_e from 100–280 °C, despite the crystal/crystal transitions at 19, 30, and 125 °C, and T_g at 125 °C. At $T_e \geqslant 280$ °C, the ductility increased rapidly with increasing temperature up to near the T_m. In this range, the EDR_{max} was 60 for extrusion at $T_e = 330$–340 °C. This excellent drawability was completely lost on attempted draw above the T_m. The structure and properties of drawn products were complexely affected by EDR and T_e. The flexural modulus, which was sensitive to the test temperatures, increased rapidly with EDR in the lower region, reached a maximum at EDR 30–40, and finally decreased above a specific EDR, which depended on the T_e. At EDRs above the specific EDR, a flaw was generated in the extrudate. The crystallite size along the chain axis D_{0015}, determined by WAXD, correlated well with the complex changes of modulus with EDR at a given T_e, as we have found previously in superdrawing of ultrahigh molecular weight polyethylene single-crystal mats. The crystallite size D_{100} of ~ 45 nm, which corresponds to the lateral dimension of microfibrils of highly drawn PTFE, was significantly larger than those generally found in other polymers. The optimization of the extrusion draw conditions resulted in a maximum flexural modulus at 24 °C of 20 GPa at an EDR of 40 for a T_e of 340 °C. This modulus is ten times higher than the tensile modulus previously reported.

Acknowledgement

The authors thank Mr Takatoshi Nishizawa, Oji-Yuka Synthetic Paper Co. Ltd, for his help in obtaining the scanning electron micrographs.

References

1. A. E. ZACHARIADES and R. S. PORTER (eds), "Strength and Stiffness of Polymers", Plastic Engineering Series, Vol. 4 (Marcel Dekker, New York, 1983).
2. I. M. WARD (ed.), "Development in Oriented Polymers-2" (Elsevier Applied Science, London, 1987).
3. A. E. ZACHARIADES and R. S. PORTER (eds), "High Modulus Polymers", Plastic Engineering Series, Vol. 17 (Marcel Dekker, New York, 1988).
4. T. KANAMOTO and R. S. PORTER, in "Integration of Fundamental Polymer Science and Technology", edited by P. J. Lemstra and L. A. Kleintjens (Elsevier Applied Science, 1989) p. 168.
5. J. SMOOK and J. PENNINGS, *Coll. Polym. Sci.* **262** (1984) 712.
6. P. J. BARHAM and A. KELLER, *J. Mater. Sci.* **20** (1985) 2281.
7. K. FURUHATA, T. YOKOKAWA, C. SEOUL and K. MIYASAKA, *J. Polym. Sci. Polym. Phys. Ed.* **24** (1986) 59.
8. N. A. J. M. VAN AERLE, PhD dissertation, Eindhoven University of Technology, The Netherlands (1989).
9. N. GERRITS, PhD dissertation, Eindhoven University of Technology (1990).
10. P. SMITH, P. J. LEMSTRA, B. CALB and A. J. PENNINGS, *Polym. Bull.* **1** (1979) 733.
11. P. SMITH, H. D. CHANZY and B. P. ROTZINGER, *Polym. Commun.* **26** (1985) 258.
12. B. P. ROTZINGER, H. D. CHANZY and P. SMITH, *Polymer* **30** (1989) 1814.
13. A. E. ZACHARIADES, M. P. C. WATTS, T. KANAMOTO and R. S. PORTER, *J. Polym. Sci. Polym. Lett. Ed.* **17** (1979) 487.
14. G. T. PAWLIKOWSKI, D. J. MITCHELL and R. S. PORTER, *J. Polym. Sci. Polym. Phys. Ed.* **26** (1988) 1865.
15. T. KANAMOTO, T. OHAMA, K. TANAKA, M. TAKEDA and R. S. PORTER, *Polymer* **28** (1987) 1617.
16. T. KAMEDA and T. KANAMOTO, *Polym. Prep. Jpn* **42** (1993) P-1478.
17. F. J. RAHL, M. A. EVANCO, R. J. FREDERICKS and A. C. REIMSCHUESSEL, *J. Polym. Sci. A-2* **10** (1972) 1337.
18. S. YAMAGUCHI, *Kobunshi Ronbunshu* **39** (1982) 493.
19. T. FOLDA, H. HOFFMAN, H. CHANZY and P. SMITH, *Nature* **333** (6168) (1988) 55.
20. H. W. STARKWEATHER Jr, *J. Polym. Sci. Polym. Phys. Ed.* **17** (1979) 73.
21. R. L. M. GEE and J. R. COLLIER, *Polym. Eng. Sci.* **26** (1986) 239.
22. Mitsui/Du Pont Fluorochemicals Co. Ltd (1993).
23. M. KAKUDO and N. KASAI, "X-Ray Diffraction of Polymers" (Maruzen, Tokyo, 1968).
24. A. L. RYLAND, *J. Chem. Educ.* **35** (1958) 80.
25. C. A. SPERATI and H. W. STARKWEATHER Jr, *Adv. Polym. Sci.* **2** (1961) 465.
26. A. J. WADDON and A. KELLER, *J. Polym. Sci. Polym. Phys. Ed.* **28** (1990) 1063.
27. *Idem, ibid.* **30** (1992) 923.
28. S. M. AHARONI and J. P. SIBILIA, *J. Appl. Polym. Sci.* **23** (1979) 133.
29. T. NISHINO, PhD dissertation, Kobe Univeristy (1990).
30. T. YAMAMOTO and T. HARA, *Polymer* **23** (1982) 521.
31. E. S. CLARK and L. T. MUUS, *Z. Kristallogr.* **117** (1962) 119.
32. D. M. SADLER and P. J. BARHAM, *Polymer* **31** (1990) 36.
33. *Idem, ibid.* **31** (1990) 42.
34. *Idem, ibid.* **31** (1990) 46.
35. A. G. GIBSON, G. R. DAVIES and I. M. WARD, *ibid.* **19** (1978) 683.
36. A. TSURUTA, T. KANAMOTO, K. TANAKA and R. S. PORTER, *J. Polym. Sci. Polym. Phys. Ed.* **23** (1985) 429.
37. K. O'LEARY and P. H. GEIL, *J. Appl. Phys.* **38** (1967) 4169.
38. K. SAKAOKU and A. PETERLINE, *J. Polym. Sci. A-2* **9** (1971) 895.
39. M. G. DOBB and D. J. JOHNSON, in "Development in Oriented Polymers", edited by I. M. Ward (Elsevier Applied Science, London, 1987) Ch. 4.
40. J. R. MINTER, K. SHIMAMURA and E. L. THOMAS, *J. Mater. Sci.* **16** (1981) 3303.
41. A. J. OWEN, in "Development in Oriented Polymers", edited by I. M. Ward (Elsevier Applied Science, London, 1987) Ch. 7.
42. H. H. CHUAH, R. S. PORTER, and J. S. LIN, *ibid.* **19** (1986) 2732.

Received 13 October 1993
and accepted 9 June 1994